PHYSICAL REVIEW E 78, 066108 (2008)

Duration of transient fronts in a bistable reaction-diffusion equation in a one-dimensional bounded domain

Yo Horikawa*
Faculty of Engineering, Kagawa University, Takamatsu, 761-0396, Japan
(Received 3 May 2008; revised manuscript received 24 September 2008; published 17 December 2008)

The duration of transient fronts in a bistable reaction-diffusion equation in a bounded domain is considered. The speed of the front decreases exponentially with the length of the domain, and the duration increases exponentially with the domain length. The duration of the fronts generated from random initial conditions is distributed in a power-law form up to a cutoff time. The cutoff time then increases exponentially with the domain length so that the power-law distribution dominates for large domains. Further, external noise of intermediate strength increases the mean duration of the fronts. The increases in the duration with the domain length become almost linear, however, in the presence of asymmetry in the cubic nonlinearity.

DOI: 10.1103/PhysRevE.78.066108 PACS number(s): 82.40.Ck, 05.45.−a, 47.54.−r, 05.40.−a

I. INTRODUCTION

Traveling fronts in reaction-diffusion systems have been of wide interest in various fields: e.g., combustion, chemical reaction, cell biology, nerve spike propagation, ecological systems, and population dynamics [1–6]. Studies on traveling fronts in reaction-diffusion equations originated from Luther (1906), Fisher (1937), and Kolmogoroff, Petrovsky, and Piscounoff (1937) (see [4]), in which a scalar monostable equation with quadratic nonlinearity in a one-dimensional domain was dealt with. Then, various systems including bistable, multivariable, discrete, and two- or three-dimensional systems have been studied and the existence and stability of traveling front solutions have been proven [6]. Further, various properties of front solutions have been shown even in simple scalar reaction-diffusion equations in a one-dimensional space: e.g., pinning of fronts with inhomogeneity [7,8], noise-induced front propagation [9,10], propagation failure in discrete systems [11], fronts of algebraically decaying form [12], finite-time extinction of fronts [13], and sharp transitions between extinction and propagation of fronts [14].

Of interest is the movement and interaction of fronts or kinks in bistable reaction-diffusion equations with cubic nonlinearity. It is known that the speeds of the fronts are extremely small and decrease exponentially with the distance to the boundaries or the distance between the fronts in a one-dimensional domain ([15–17] and references in [18]). These slowly evolving states are referred to dynamical metastability or metastable dynamics [18]. The fronts are transient and annihilate through collisions to the boundaries or with each other, but their duration increases exponentially with the length of the domain. Further, the number, density, and distance of the fronts decrease only logarithmically in time when fronts are randomly distributed initially in the domain [19,20]. That is, the transient time from an initial state to one of the stable states increases exponentially with the size of the domains.

Such exponential dependences of transient time on system size have attracted much attention in the field of dissipative nonlinear systems. The dependences have been found in transient spatiotemporal chaos in coupled map lattices [21] and reaction-diffusion equations [22], the length and number of cycles in transient states in asymmetric neural networks [23], transient irregular firings in diluted inhibitory networks of pulse-coupled neurons [24], transient well-controlled sequences in continuous-time Hopfield networks with Liapunov functions [25], and transient oscillations in unidirectionally coupled ring neural networks [26,27]. These systems never reach their stable states in a practical time when the system size is sufficiently large. The transient states thus play more important roles than the asymptotic states in actual systems: e.g., information processing in the nervous systems.

In this paper, the duration of transient fronts in a scalar bistable reaction-diffusion equation in a bounded domain is studied. In Sec. II, the model equation and a kinematic description of the movement of the fronts are shown. Properties of the duration of the transient fronts are then derived and compared with the results of computer simulation in Sec. III. It is then shown that the duration of the fronts generated from random initial conditions is distributed in a power-law form up to a cutoff time, which increases exponentially with the length of a domain. Further, effects of external noise on the transient time are examined in Sec. IV and it is shown that the duration of the fronts increases in the presence of noise of intermediate strength. Effects of asymmetry in the cubic nonlinearity are also considered in Sec. V and it is shown that shifts in one of the stable states degrade the exponential increases in the duration of the fronts with the domain length so that the increases become almost linear. The conclusion and a discussion are given in Sec. VI. In the Appendix, an intuitive derivation of the kinematics for the movement of the fronts is noted.

II. MODEL EQUATION AND FRONT KINEMATICS

We consider the following initial-boundary value problem of a scalar reaction-diffusion equation in a one-dimensional bounded domain:

$$\partial u/\partial t = \partial^2 u/\partial x^2 + f(u), \quad -l/2 < x < l/2 \quad (l > 0),$$

$$f(u) = -(u-u_1)(u-u_2)(u-u_3),$$

*horikawa@eng.kagawa-u.ac.jp

$$u_1 = -1, \quad u_2 = 0, \quad u_3 = 1,$$

$$u(x,0) = \varphi(x), \quad \partial u(-l/2,t)/\partial x = \partial u(l/2,t)/\partial x = 0. \quad (1)$$

The values $u_1=0$ and $0<u_2<1$ have been often used, but we use this form for later analysis. There are three spatially homogeneous solutions: $u(x,t)=u_1$, u_3, which are stable, and u_2 unstable. This bistable model is referred to as the heterozygote inferiority class in the field of population genetics [1]. The equation is called the time-dependent Ginzburg-Landau equation [28] and the Schlögl model [9] in the field of phase transitions. Propagating fronts with this cubic kinetics were first studied by Semenov *et al.* in 1939, which is noted in [5]. There is a stable traveling front $u(z)$ in an infinite domain $-\infty<x<\infty$[4], which connects the two stable states u_1 and u_3 as

$$u(x,t) = u(z), \quad z = x - ct, \quad u(-\infty) = u_1, \quad u(\infty) = u_3,$$

$$u(z) = \{u_3 + Ku_1 \exp[(u_1 - u_3)z/\sqrt{2}]\}/\{1 + K \exp[(u_1 - u_3) \times z/\sqrt{2}]\} = \tanh(z/\sqrt{2}) \quad (K = 1),$$

$$c = (u_1 - 2u_2 + u_3)/\sqrt{2} = 0, \quad (2)$$

where K is an arbitrary constant and is set to 1 so that $u(0)=0$. For the values of u_i in Eq. (1), the speed c is zero and the front is stationary.

In a bounded domain $-l/2<x<l/2$ in Eq. (1), the following stationary standing front solution exists, but is unstable:

$$u(-l/2,t) = -m, \quad u(0,t) = 0, \quad u(l/2,t) = m \quad (0 < m < 1),$$

$$m = \sqrt{2 - \frac{1}{1 - 8\exp(-l/\sqrt{2})}} \approx 1 - \delta, \quad (3)$$

$$\delta = 4\exp\left(\frac{-l}{\sqrt{2}}\right), \quad l \gg 1.$$

The derivation of the values m at the boundaries is given in the Appendix. The solution $u(x,t)$ of Eq. (1) then converges to one of the steady states u_1 and u_3. However, it has been shown that the instability of the stationary fronts weakens exponentially with the domain length l through the eigenvalue problem [16]. This results in the exponentially slow movement of the fronts. Let one front be located at $x=l/2-l_+$, and let l_+ be the length of the right domain in which $u\geqslant 0$ and then $l-l_+$ be the length of the left domain in which $u<0$—i.e., $u<0$ for $-l/2<x<l/2-l_+$, $u=0$ at $x=l/2-l_+$, and $u>0$ for $l/2-l_+<x<l/2$. The movement of the front is expressed by [15–17]

$$dl_+/dt \approx k\{\exp[-\alpha(l - l_+)] - \exp(-\alpha l_+)\},$$

$$k = 24/\sqrt{2} \approx 17.0, \quad \alpha = 2\sqrt{2} \approx 2.83. \quad (4)$$

When the length l_+ is smaller than $l/2$—i.e., the front is located at $x>0$—the sign of the right-hand side of Eq. (4) is negative so that l_+ becomes zero and the front moves toward the right boundary $x=l/2$ and vice versa. However, the speed of the front is proportional to the difference between the inverses of the exponentials of the two lengths $(\exp(-l_+)-\exp[-(l-l_+)])$, not the inverse of the exponential of the difference between the lengths $(\exp(-l_+)-\exp[-(l-l_+)])$. Then the speed decreases exponentially with the total length of the domain even though the difference between the two lengths is fixed.

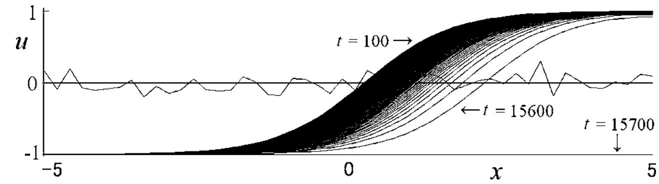

FIG. 1. Time course of $u(x,t)$ under a random initial condition. Plotted are snapshots of u at intervals of $t=100$.

This extremely slow movement of the fronts and their long duration are easily seen with computer simulation. Here Eq. (1) was discretized with $\Delta x=0.2$ and $\Delta t=0.01$, and the length l of the domain was set to 10. The explicit finite-difference method was used for numerical integration. The initial value $\varphi(x)$ at each x was drawn from Gaussian white noise with the mean 0 and standard deviation 0.1. It was confirmed that finer space and time steps give about the same results. Figure 1 shows an example of the time course of $u(x,t)$, in which snapshots of u at intervals of $t=100$ are plotted. An irregular line around $u=0$ corresponds to the random initial values $\varphi(x)$, and a front is formed in a short time. The almost black region corresponds to the slow movement of the front, and it takes about $t=15\,500$ for u to converge to u_1.

III. DURATION OF TRANSIENT FRONTS

Exponential increases in the duration of the transient fronts with the domain length have been proven in a general form in [16], in which the upper and lower bounds of the duration were given carefully considering the accuracy of the equations of the front positions. We here derive properties of the duration of the fronts in Eq. (1) by directly using Eq. (4) in the same way as [27].

A. Duration of rectangular fronts

Equation (4) with the initial value $l_+(0)=l_0$ is solved by substituting $y=\exp(\alpha l_+)$ as

$$dy/dt = \alpha k[\exp(-\alpha l)y^2 - 1], \quad y(0) = \exp(\alpha l_0), \quad l_+(0) = l_0, \quad (5)$$

$$\exp[-\alpha l_+(t)] = \exp(\alpha l/2)\tanh(-\exp(-\alpha l/2)\alpha kt + \operatorname{arctanh}\{\exp[\alpha(l_0 - l/2)]\}), \quad (6)$$

where k and α are the same as in Eq. (4). We assume $l_0 \leqslant l/2$ without any restriction. The solution $l_+(t)$ explodes to minus infinity in a finite time at which the augment of the hyperbolic tangent becomes zero. The duration T of the transient fronts is given by setting $l_+(T)=0$ as

$$T = \frac{\exp(\alpha l/2)}{\alpha k}(\mathrm{arctanh}\{\exp[\alpha(l_0 - l/2)]\} - \mathrm{arctanh}[\exp(-\alpha l/2)]). \tag{7}$$

The duration T increases exponentially with the domain length l. Further, it increases exponentially as the initial length l_0 when l is large since $\mathrm{arctanh}(x) \approx x$ for small x. A simpler form of the duration $T(l_0)$ for large l is derived by letting l be infinity in Eq. (4). The equation and the solution become

$$dl_+/dt = -k\exp(-\alpha l_+),$$

$$l_+(t) = \frac{\ln[\exp(\alpha l_0) - \alpha k t]}{\alpha},$$

$$T = \frac{\exp(\alpha l_0) - 1}{\alpha k}, \quad l_+(0) = l_0 \quad l_+(T) = 0 \quad (0 \leqslant l_0 \leqslant l/2). \tag{8}$$

This shows the exponential increases in the duration T with the initial length l_0. Further, the length decreases in proportion to time in the beginnings—i.e., $l_0 - l_+(t) \approx k\exp(-\alpha l_0)t$ for $t \ll \exp(\alpha l_0)/(\alpha k)$, and the decrease rate decreases exponentially with the initial length.

To confirm this, a computer simulation was done with Eq. (1) under the initial conditions

$$\varphi(x) = -1 \quad (-l/2 < x < l/2 - l_0) = 1 \quad (l/2 - l_0 \leqslant x < l/2), \tag{9}$$

where $l = 15$. That is, the initial pattern $\varphi(x)$ is a rectangular front with the lengths l_0 and $l - l_0$, and it quickly becomes a traveling front. Then l_0 is considered to be the initial value of l_+ [$l_+(0) = l_0$]. The transient time T of u to $u_1(=-1)$ was measured with the condition $|u(x,T) - u_1| < 0.1$ for $-l/2 < x < l/2$. Figure 2 shows the duration T against the initial length l_0 ($0.2 \leqslant l_0 \leqslant 7.4$), in which the simulation results (solid circles), Eq. (7) (solid line) and Eq. (8) (dashed line), are plotted. Equations (7) and (8) hardly differ, and they agree with the simulation results except for small l_0 ($\leqslant 2.0$).

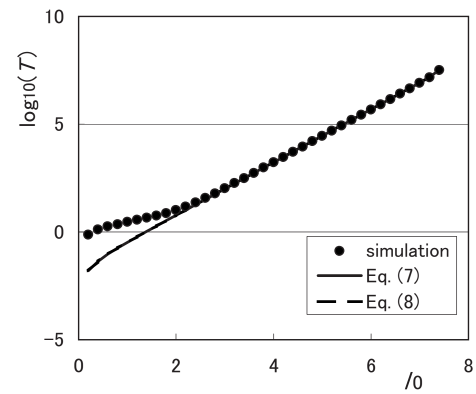

FIG. 2. Duration T of the transient front vs initial length l_0 of the right domain ($0.2 \leqslant l_0 \leqslant 7.4$) in a domain of length $l = 15$. Simulation results (solid circles), Eq. (7) (solid line), and Eq. (8) (dashed line).

B. Distribution of duration under random initial conditions

When the initial values $\varphi(x)$ are given randomly independently of x, the initial length l_0 of the smaller domain of the generated front is considered to be distributed uniformly in $0 \leqslant l_0 \leqslant l/2$. Then the probability density function $h(T)$ of the duration T of the transient fronts (the convergence time of u to u_1 or u_3) is derived with

$$\int_0^{l_0} U(0,l/2)dl_0' = \int_0^T h(T')dT', \tag{10}$$

where $U(a,b)$ is the uniform distribution between a and b. Hence we obtain

$$h(T) = \frac{1}{|dT(l_0;l)/dl_0|}\frac{2}{l} = \left|\frac{dl_0(T;l)}{dT}\right|\frac{2}{l} = \left|\frac{d[\ln(\tanh\{\exp(-\alpha l/2)\alpha k T + \mathrm{arctanh}[\exp(-\alpha l/2)]\})/\alpha]}{dT}\right|\frac{2}{l}$$
$$= 4k\exp(-\alpha l/2)\mathrm{cosech}(2\{\exp(-\alpha l/2)\alpha k T + \mathrm{arctanh}[\exp(-\alpha l/2)]\})/l. \tag{11}$$

There is a cutoff point $T_c = \exp(\alpha l/2)/(\alpha k)$ at which the form of $h(T)$ changes. On the one hand, for $T < T_c$ or when the domain length l is large, the approximate form is derived by using $\mathrm{arctanh}(x) \approx x$ and $\sinh(x) \approx x$ for $x \ll 1$:

$$h(T) \approx \frac{k}{\alpha k T + 1}\frac{2}{l} \quad (0 \leqslant T \leqslant [\exp(\alpha l/2) - 1]/(\alpha k)). \tag{12}$$

This is also derived from Eq. (8), in which l is set to be infinity. The probability density function is approximated by a power-law distribution. On the other hand, for $T > T_c$ or when l is small, the probability density function is approximated by the exponential distribution by using $\sinh(x) \approx \exp(x)/2$ ($x \gg 1$) for large T in Eq. (11):

$$h(T) \approx \lambda\exp(-\lambda T), \quad \lambda \approx 2\alpha k\exp(-\alpha l/2) \quad (T \geqslant 0). \tag{13}$$

The cutoff point increases exponentially with the domain length and the region in which the duration is distributed in the power-law form extends. The proportion of the duration over the cutoff is evaluated as $\mathrm{Prob}\{T > T_c\}$

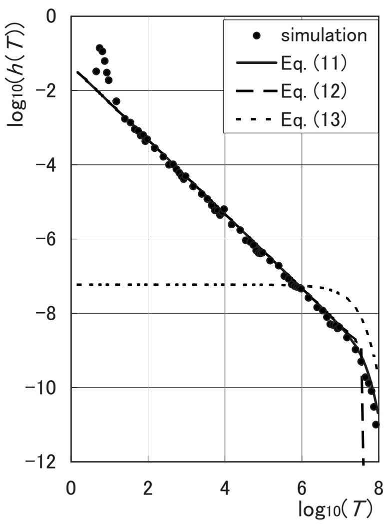

FIG. 3. Probability density function h of duration T of transient fronts in a domain of length $l=15$. Plotted are a normalized histogram of the duration of 10 000 transient fronts obtained with computer simulation of Eq. (1) under the Gaussian random initial condition $\varphi(x) \sim N(0,0.1^2)$ (solid circles), Eq. (11) (solid line), Eq. (12) (dashed line), and Eq. (13) (dotted line).

$\approx 2^{1/2}\exp(-2)/l \approx 0.19/l$, which decreases in proportion to the inverse of the domain length.

Figure 3 shows the probability density function h of the duration T of the transient fronts in the domain of length $l = 15$. Plotted is a normalized histogram of the duration of 10 000 transient fronts obtained with computer simulation of Eq. (1) (solid circles). The initial values $\varphi(x)$ are given by random numbers with the Gaussian function of mean 0 and standard deviation 0.1. The histogram of the simulation results is composition of those made per decade. The slope of the log-log graph of the histogram is close to −1, and the density decreases with the inverse of T up about to the cutoff point $T_c \approx 3.4 \times 10^7$ obtained with Eq. (11). Equation (11) (solid line), Eq. (12) (dashed line), and Eq. (13) (dotted line) are also plotted. Equation (11) agrees with the simulation results for the whole region, while Eq. (12) agrees with them for $T < T_c$.

The mean m, the variance σ^2, and the coefficient of variation C_V of the duration T are calculated with $h(T)$. Using Eqs. (8) and (12) for large l, they are expressed as

$$m(T(l)) = 2[\exp(\alpha l/2) - \alpha l/2 - 1]/(\alpha^2 k l),$$

$$\sigma^2(T(l)) = [\exp(\alpha l) - 4\exp(\alpha l/2) + \alpha l + 3]/(\alpha^3 k^2 l) - [m(T(l))]^2,$$

$$C_V(T(l)) = \sigma(T(l))/m(T(l)) \approx \sqrt{\alpha l}/2 \quad (l \gg 1). \tag{14}$$

Thus the mean and standerd deviction (σ) increase exponentially with αl and the relative variation (C_V) increases as $2^{-1/4} l^{1/2}$. Figure 4 shows a semilogarithmic plot of the mean m against the domain length l, in which the simulation results of 10 000 runs for each l (solid circles), the numerical calculations with $h(T)$ in Eq. (11) (solid line) and Eq. (14)

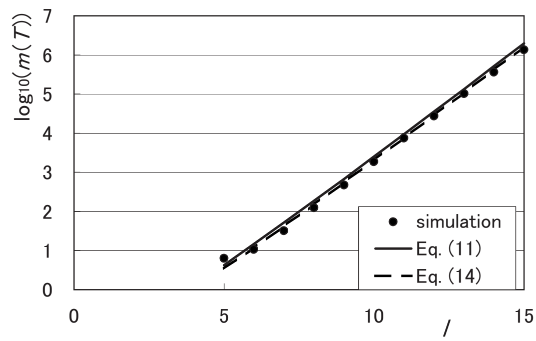

FIG. 4. Mean duration m of transient fronts vs domain length l. Simulation results (solid circles), numerical calculation with $h(T)$ in Eq. (11) (solid line) and Eq. (14) (dashed line).

(dashed line), are plotted. Equations (11) and (14) agree with the simulation results, although they are slightly large.

C. Transient time in two-dimensional domains

Dependences of the transient time on the domain size in two-dimensional domains are considered. A computer simulation in a rectangular domain under random initial conditions and the Neumann boundary condition was done. Figure 5 shows a normalized histogram h of the transient time T of $u(x,y,t)$ of 10 000 runs obtained with the simulation in a two-dimensional square domain $-l/2 < x < l/2$, $-l/2 < y < l/2$ $(l=10)$ (solid circles). The initial condition $u(x,y,0)$ is drawn from the Gaussian distribution $N(0,0.1^2)$. The probability density functions obtained in a one-dimensional domain of length $l=10$ are also plotted: Eq. (11) (solid line),

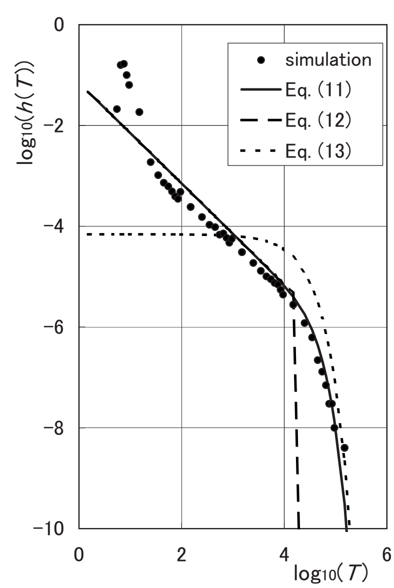

FIG. 5. Normalized histogram h of the transient time T of $u(x,y,t)$ in a two-dimensional domain $-l/2 < x < l/2$, $-l/2 < y < l/2$ $(l=10)$ obtained with computer simulation under Gaussian random initial condition $N(0,0.1^2)$ (solid circles). Equation (11) (solid line), Eq. (12) (dashed line), and Eq. (13) (dotted line) are also plotted for $l=10$.

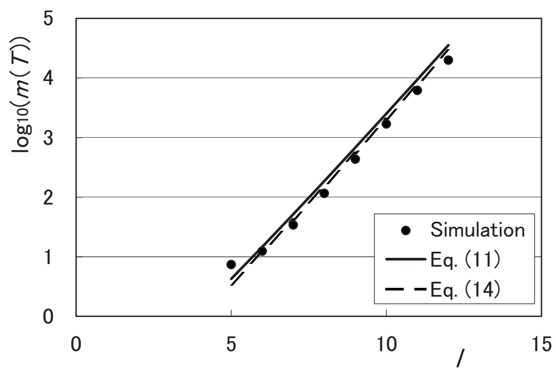

FIG. 6. Mean of 10 000 transient times obtained with computer simulation in a two dimensional domain $-l/2<x,\ y<l/2$ for $5 \leqslant l \leqslant 12$ (solid circles), mean transient time calculated with Eq. (11) (solid line) and Eq. (14) (dashed line).

Eq. (12) (dashed line), and Eq. (13) (dotted line). Here the value of the cutoff point is $T_c \approx 2.9\times 10^4$, and Eq. (11) agrees with the simulation results. Figure 6 shows the mean of 10 000 transient times obtained with the simulation for $5 \leqslant l \leqslant 12$ (solid circles). The mean transient time calculated with Eqs. (11) and (14) is also plotted with solid and dashed lines, respectively, and they agree with the simulation results. The expressions for one-dimensional domains of length l agree with the simulation results in two-dimensional squares of the same length l of their sides. The exponential increases in the transient time are intrinsically one-dimensional effects, and the transient time depends on not the area, but the length of the domain.

IV. EFFECTS OF EXTERNAL NOISE

It is known that external spatiotemporal noise and variations in parameter values cause deviation and fluctuations in the speeds of the fronts in bistable reaction-diffusion equations [7–10]. Then the duration of the transient fronts varies in the presence of noise. Effects of additive white noise on the duration are considered with the following stochastic differential equation for the first equation in Eq. (1):

$$\partial u/\partial t = \partial^2 u/\partial x^2 + f(u) + \sigma_x n(x,t), \quad -l/2 < u < l/2 \quad (l>0),$$

$$E\{n(x,t)\}=0, \quad E\{n(x,t)n(x',t')\} = \delta(x-x')\delta(t-t'), \tag{15}$$

where $n(x,t)$ is spatiotemporal Gaussian white noise and σ_x is the strength of the noise. The noise $\sigma_x n(x,t)$ gives random fluctuations in the speed of the front. The movement of the front is approximated by adding a noise term to the kinematic equation (4) as

$$dl_+/dt = k\{\exp[-\alpha(l-l_+)] - \exp(-\alpha l_+)\} + \sigma_l n(t),$$

$$\sigma_l^2 \approx \int_{-l/2}^{l/2} (\sigma_x du/dz)^2 dz \Bigg/ \left(\int_{-l/2}^{l/2} (du/dz)^2 dz\right)^2$$
$$\approx \sigma_x^2 \Bigg/ \int_{-l/2}^{l/2} (du/dz)^2 dz$$
$$\approx \sigma_x^2 \Bigg/ \int_{-\infty}^{\infty} [\mathrm{sech}^2(z/\sqrt{2})/\sqrt{2}]^2 dz$$
$$= \sqrt{9/8}\,\sigma_x^2,$$

$$E\{n(t)\}=0, \quad E\{n(t)n(t')\} = \delta(t-t'), \tag{16}$$

where $n(t)$ is Gaussian white noise in time. The strength σ_l ($\approx 1.03\sigma_x$) of the noise in Eq. (16) takes about the same value as σ_x in Eq. (15) for this simple additive noise [9]. The duration T of the transient fronts is evaluated with the first passage time (FPT) of l_+ from l_0 to 0 or l [$l_+(0)=l_0$, and $l_+(T)=0$ or l] in the same way as [31].

We can consider the FPT from l_0 to 0 by letting $l_+<l/2$ and adding a reflecting boundary at $l_+=l/2$ owing to the symmetry instead of both absorbing boundaries at $l_+=0$ and l. The mean $m(T(l_0))$ and variance $\sigma^2(T(l_0))$ of the FPT are then given by [32]

$$m(T;0|l_0) = 2\left(\int_0^{l_0} \pi(\eta)d\eta \int_\eta^{l/2} [\sigma_l^2 \pi(\xi)]^{-1} d\xi\right),$$

$$\sigma^2(T) = 4\left(\int_0^{l_0} \pi(\eta)d\eta \int_\eta^{l/2} m(T;0|l_0)/[\sigma_l^2\pi(\xi)]^{-1} d\xi\right) - m(T;0|l_0)^2,$$

$$\pi(y) = \exp\left(-\int^y \frac{2a(\eta)}{\sigma_l^2} d\eta\right), \tag{17}$$

$$a(y) = k\{\exp[-\alpha(l-y)] - \exp(-\alpha y)\}.$$

When the domain length is large, the FPT problem of simpler form is given by letting $a(l)$ be $-k\exp(-\alpha l_+)$ in Eq. (17). Figure 7 shows the mean $m(T(l_0))$ of the duration of the transient fronts when $l=10$ and $l_0=4$. The mean of 1000 runs of computer simulation with Eqs. (1) and (15) under the initial condition, Eq. (9), of rectangular fronts are plotted with solid circles. The mean duration increases at the intermediate noise strength, and the fluctuations caused by the intermediate noise tend to increase the FPT. In the simple Ornstein-Uhlenbeck process, the deterministic term is linear and the noise always decreases the FPT. The increases in the duration of the transient fronts are due to the nonlinear exponential terms in Eq. (4). That is, the ratio of the increase $T(l_+ + \Delta l) - T(l_+)$ due to a small positive fluctuation Δl in l_+ to the decrease $T(l_+) - T(l_+ - \Delta l)$ due to a negative fluctuation $-\Delta l$ is always larger than 1—i.e., $dT/dl_+ > 0$ and $d^2T/dl_+^2 > 0$. Thus the fluctuations caused by the noise of small strength tend to increase the FPT. As the noise strength increases, the effects of the diffusion become dominant and the FPT decreases to the order of l^2. The FPT obtained by numerically integrating Eq. (17) is plotted with a solid line, and

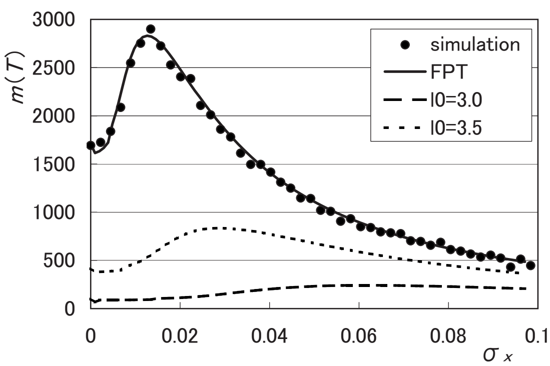

FIG. 7. Mean duration m of transient fronts with initial length l_0 of right domain vs standard deviation SD σ_x of external noise ($l=10$, $l_0=4$). Simulation results (solid circles), FPT with numerical integration of Eq. (17) (solid line). FPT with Eq. (17) for $l_0=3.0$ and 3.5 is also plotted with dashed and dotted lines, respectively.

it agrees with the simulation results (solid circles). The FPT calculated with the equation $a(l)=-k\exp(-\alpha l_+)$ hardly differs from them (data not shown). Note that the decreases in the FPT at small noise strength ($\sigma_x \approx 0.002$) may be an artifact due to the instability of the numerical integral since they do not appear in the simulation.

The peak of the mean duration moves toward the region of large noise strength, and the value decreases as the initial length l_0 decreases and vice versa. Numerical integrals of Eq. (17) for $l_0=3.0$ and 3.5 are also plotted with dashed and dotted lines, respectively, in Fig. 7. When $l_0=l/2$, the standing fronts remain stationary in the absence of noise and the duration of the fronts is considered to decrease monotonically as the noise strength increases. Under random initial conditions for u, the mean duration of the fronts is approximated by the mean of $T(l_0)$ over $0<l_0<l$. The duration for the initial length l_0 close to $l/2$ mainly contributes to it, and it can be shown with computer simulation and numerical integrals with Eq. (17) that the mean duration monotonically decreases with the noise strength.

V. EFFECTS OF ASYMMETRY IN THE CUBIC NONLINEARITY

When the cubic function f is not symmetric—i.e., $|u_1| \neq |u_3|$ or $u_3-u_2 \neq u_2-u_1$—unstable stationary front solutions never exist. There is a stable traveling front in an infinite domain with nonzero speed c given by Eq. (2). Intuitively, when $u_1=-1$ and $u_3=1-\delta$, the speed is approximated by $c \approx -2^{-1/2}\delta$ and this constant speed bounds the duration of the fronts to $|l/c| \approx 2^{1/2} l/\delta$ in a domain of length l.

An expression for the movement of the transient fronts for $u_3=1-\delta$ is derived in the same way as the Appendix as follows:

$$dl_+/dt \approx c_0 + k\{\exp[-\alpha'(l-l_+)] - \exp(-\alpha l_+)\} + o(\delta^2),$$

$$c_0 \approx \delta/\sqrt{2} - 3\delta^2/(2\sqrt{2}) \approx \delta/\sqrt{2}, \quad (18)$$

$$\alpha' = \alpha(1-\delta) \approx \alpha \quad (\delta \ll 1).$$

We here put $c_0=2^{-1/2}\delta$ and $\alpha'=\alpha$ for small $|\delta|$ for simplicity. There are the following critical length l_c and shift δ_c, below which the front moves right and the length l_+ of the right domain of the front decreases to zero and over which the front moves left and l_+ increases to l:

$$l_c = \ln\{2/[c_0/k + \sqrt{(c_0/k)^2 + 4\exp(-\alpha l)}]\}/\alpha,$$

$$\delta_c = \sqrt{2}k\{\exp(-\alpha l_+) - \exp[-\alpha(l-l_+)]\}. \quad (19)$$

The duration of the fronts with the initial length $l_+(0)=l_0$ is obtained as

$$T_1 = \ln[A(0)/A(l_0)]/[k\alpha\sqrt{(c_0/k)^2 + 4\exp(-\alpha l)}]$$

$$[l_0 < l_c,\ l_+(T_1)=0],$$

$$T_2 = \ln[A(l)/A(l_0)]/[k\alpha\sqrt{(c_0/k)^2 + 4\exp(-\alpha l)}]$$

$$[l_0 > l_c,\ l_+(T_2)=l],$$

$$A(l') = \frac{\exp(-\alpha l') - [c_0/k + \sqrt{(c_0/k)^2 + 4\exp(-\alpha l')}]}{\exp(-\alpha l') - [c_0/k - \sqrt{(c_0/k)^2 + 4\exp(-\alpha l')}]}. \quad (20)$$

Simpler forms of them are given by letting l be infinity in Eq. (18) as

$$dl_+/dt \approx c_0 - k\exp(-\alpha l_+),$$

$$l_c = \ln(k/c_0)/\alpha = \ln(\sqrt{2}k/\delta)/\alpha, \quad \delta_c = \sqrt{2}k\exp(-\alpha l_+),$$

$$T_1 = \ln\{(1-c_0/k)/[1-c_0/k\exp(\alpha l_0)]\}/(\alpha c_0)$$

$$[l_0 < l_c,\ l_+(T_1)=0],$$

$$T_2 = \ln\{[c_0/k\exp(\alpha l) - 1]/[c_0/k\exp(\alpha l_0) - 1]\}/(\alpha c_0)$$

$$[l_0 > l_c,\ l_+(T_2)=l]. \quad (21)$$

For a fixed small shift $0<\delta \ll 1$ in u_3, the duration T_1 increases exponentially with l_0 when $l_0<l_c$ and becomes infinity at $l_0=l_c$. Then T_2 decreases almost linearly with l_0 when $l_0>l_c$:

$$T_1 \approx [\exp(\alpha l_0) - 1]/(\alpha k) \quad (0 < l_0 < l_c)$$

$$\to \infty \quad (l_0 \to l),$$

$$T_2 \approx (l-l_0)/c_0 = \sqrt{2}(l-l_0)/\delta \quad (l_c < l_0 < l-l_c)$$

$$\approx [\exp(\alpha(l-l_0)) - 1]/(\alpha k) \quad (l-l_c < l_0 < l). \quad (22)$$

For a fixed initial length l_0, the duration T_1 increases monotonically with δ and becomes infinity at $\delta=\delta_c$. Then T_2 decreases in proportion to the inverse of δ. Figure 8 shows the duration T of the transient fronts against the initial length l_0

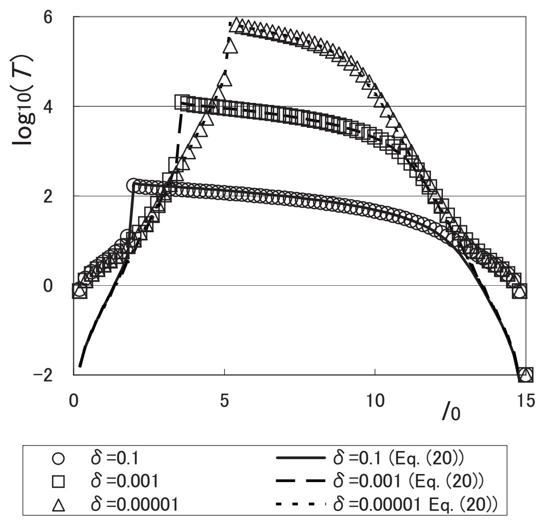

FIG. 8. Duration T of the transient front vs initial length l_0 ($0<l_0<l=15$) in the presence of asymmetry with $u_3=1-\delta$ in $f(u)$. Simulation results (symbols) and Eq. (20) (lines) are plotted for $\delta=10^{-1}$, 10^{-3}, and 10^{-5}.

of the right domain ($0<l_0<l=15$), in which the simulation results (symbols) and Eq. (20) (lines) are plotted for $\delta=10^{-1}$, 10^{-3}, and 10^{-5} (for $\delta=0$; see Fig. 2). The duration increases exponentially with l_0 up only to $T_L \approx (k/c_0-1)/(\alpha k) \approx 2^{1/2}/(\alpha\delta)$ in the side regions $0<l_0<l_c$ and $l-l_c<l_0<l$. The increase in the duration is almost linear in the middle region $l_c<l_0<l-l_c$ and is up to $T_H \approx 2^{1/2}(l-2l_c)/\delta$. The width of the region about $l_0=l_c$ in which the duration increases over T_H is exponentially small.

Under random initial conditions for $u(x,0)=\varphi(x)$, the initial lengths l_0 of the right domain of the generated fronts are regarded to be distributed uniformly in $(0,l)$. The probability density function of the duration of the transient fronts is then given by $h(T)=(1/|dT_1/dl_0|+1/|dT_2/dl_0|)/l$. Using Eq. (22), it is approximated as

$$\begin{aligned} h(T) &\propto 1/T \quad [T<T_L \approx (k/c_0-1)/(\alpha k) \approx \sqrt{2}/(\alpha\delta)] \\ &\approx \frac{1}{T_H-T_L}\frac{l-2l_c}{l} \approx \delta/(\sqrt{2}l) \quad (T_L<T<T_H) \\ &\propto \exp(-\lambda T) \quad (T>T_H \approx \sqrt{2}(l-2l_c)/\delta \\ &= \sqrt{2}\{l-[2\ln(\sqrt{2}k/\delta)-1]/\alpha\}/\delta). \end{aligned} \tag{23}$$

The duration is uniformly distributed around l/δ in the region $T_L<T<T_H$ of width $O(l/\delta)$. The mean duration increases in proportion about to the total domain length l as $m(T)\approx(T_L+T_H)/2\approx 2^{-1/2}l/\delta$ since the probability density over T_L decreases exponentially. The exponential increases in the duration of the fronts with the domain length are then degraded in the presence of the asymmetry.

VI. CONCLUSION AND DISCUSSION

The properties of the duration of the transient fronts in the bistable scalar reaction-diffusion equation in a bounded domain were derived with the kinematic equation for the front movement. The duration of the transient front exponentially increases with the smaller length of the two sides of it since the speed is proportional to the difference between the inverses of the exponentials of the two lengths [15–18]. The mean duration of the fronts generated from random initial conditions—i.e., the transient time of the system—also increases exponentially with the length of the whole domain. The probability density function of the duration of the fronts is then approximated by the power-law distribution below the cutoff time and by the exponential distribution over it. The cutoff time increases exponentially with the domain length, and the power-law distribution dominates when the domain length is large enough. The exponential increases in the transient time with the width of the domains were also shown in two-dimensional domains with a computer simulation. Further, external noise tends to increase the duration of the transient fronts owing to the nonlinear interaction of exponential forms. Then the duration changes nonmonotonically as the strength of the noise increases. The increases in the duration become almost linear with the domain length, however, when the cubic nonlinearity is asymmetric so that small drift exists.

The kinematic equation can be applied to a circular domain $u(0,t)=u(l',t)$ or a periodic boundary condition $u(x,t)=u(x+l',t)$ with $l'=2l$. It is also applicable to transient standing pulses under the Dirichlet boundary condition $u(0,t)=u(l',t)=m$ with the same sign and traveling pulses in a circular domain in the presence of convection ($\nu\partial u/\partial x$). It is also noted that the values of the variables and parameters are scaled as follows when the diffusion coefficient is ε^2 and the function f is multiplied by b^2 in Eqs. (1):

$$u(z)=\tanh[(b/\varepsilon)2^{1/2}z], \quad \delta=4\exp[-(b/\varepsilon)l/2^{1/2}],$$

$$k=24\times 2^{-1/2}\varepsilon b, \quad \alpha=2\times 2^{1/2}(b/\varepsilon), \quad \sigma_l^2=(9/8)^{1/2}(b/\varepsilon)\sigma_x^2. \tag{24}$$

The parameter ε corresponds to the characteristic width of the fronts and domain length is scaled with it [15–18].

When the domain length is larger, it can be shown with computer simulation that many fronts are generated under random initial conditions and the fronts annihilate each other through collisions. The probability density function of distances between randomly distributed fronts in large domains—e.g., $l=1000$ in Eq. (1)—has been obtained in [19,20]. It was then shown that the mean interval increases logarithmically in time through the collisions and merging of the fronts. This agrees with the exponential increases in the duration of the fronts with the domain length shown in this study. The forms of the solutions one step before converging to u_1 or u_3 are one front or one pulse (two fronts). The duration of them is dominant in the whole transient time to the steady states since it is exponentially larger than the collision times of the previous fronts. The transient time is then approximated by the duration of the finally generated front.

Further, it is known that spatial inhomogeneity can prevent fronts from moving, called pinning [7,8,10]. The standing fronts are then stabilized depending on the spatial variations. When spatial Gaussian white noise with strength σ_u is added to $f(u)$, the variances σ_c^2 of the speed of the front due to the spatial variations is approximated by $(9/8)^{1/2}\sigma_u^2$ in the same way as Eq. (16) [9]. By using Eq. (8), it is derived that the spatial variations can localize the fronts of length l larger than $6(8/9)^{1/4}/\sigma_u$ and exponential increases in the duration T appear only up about to $(9/8)^{1/4}/(2\times 2^{1/2}\sigma_u)$.

Recently, a similar mechanism of the occurrence of the exponentially slow convergence was found in transient oscillations in unidirectionally coupled ring neural networks [27]. In the ring neural networks, each neuron is bistable and there are two stable steady states in which the states of the all neurons take the same values. However, when initial states are given randomly, the neurons are separated in two blocks; the states of the neurons are positive in one block and negative in the other block. There are inconsistencies in the signs at the boundaries between the neuron blocks, and they propagate in the direction of the coupling so that the network oscillates. The speeds of the boundaries depend on the numbers of neurons in the two blocks and are described with a kinematic equation similar to Eq. (4). Then the convergence time of the network to one of the steady states becomes exponentially long as the number of neurons in the network increases.

Mathematically, in both bistable systems, there are unstable solutions: the unstable standing fronts and unstable periodic oscillations, which correspond to the separatrixes of the two stable steady states. However, they are only one-dimensionally unstable and the systems can reach the stable steady states only through the one-dimensional movement of the fronts and boundaries. Further, their instability becomes exponentially small as the system size increases; the eigenvalue of the unstable eigenspace of the stationary solution, Eq. (3), decreases to zero exponentially with the domain length [16], and the largest eigenvalue of the Poincaré map of the unstable oscillations decreases to unity double exponentially with the number of neurons [26,27]. This leads to the exponentially slow one-dimensional movement in each system.

Phenomenologically, the speeds of the fronts depend on the values at the boundaries of the domain and can be derived with them as shown in the Appendix. The equation of the movement of the boundaries in the ring neural networks was also derived directly through the values of the states of the neurons at the boundaries between the blocks. The convergence to the steady states is intrinsically linear, and their relaxation is exponential. The degrees to which the states approach the steady states are exponentially small with the system size. The speeds of the fronts and boundaries depend on the differences between the relaxation processes to the two steady states, and then the symmetry of the bistability is necessary for the exponential increases in the transient time with system size.

APPENDIX: INTUITIVE DERIVATION OF THE KINEMATICS FOR TRAVELING FRONTS

1. Unstable stationary fronts

Consider the following boundary condition in addition to Eq. (1):

$$u(-l/2,t)=m_-, \quad u(l/2,t)=m_+ \quad (-1<m_-<0<m_+<1). \tag{A1}$$

Solutions of Eqs. (1) and (A1) connect m_- and m_+, and then a front solution increasing monotonically with respect to x from $-l/2$ to $l/2$ can exist. When the values of u at the boundaries are the same ($m_+=-m_-=m$), a stationary front solution of Eqs. (1) and (A1) is derived from the following corresponding ordinary differential equation according to [2,3]

$$d^2u/dx^2+f(u)=0,$$

$$du(-l/2,t)/dx=du(l/2,t)/dx=0,$$

$$u(-l/2,t)=-m, \quad u(l/2,t)=m \quad (0<m<1). \tag{A2}$$

This can be expressed as follows unless $du/dx\equiv 0$:

$$\frac{1}{2}\frac{d}{dx}\left(\frac{du}{dx}\right)^2+f(u)\frac{du}{dx}=0,$$

$$\left(\frac{du}{dx}\right)^2+2F(u)=2F(m), \quad F(u)=\int_0^u f(\eta)d\eta=\frac{u^2}{2}-\frac{u^4}{4},$$

$$\frac{du}{dx}=\pm\sqrt{2F(m)-2F(u)}. \tag{A3}$$

The integration constant in the right-hand side in the second equation comes from the boundary conditions in Eq. (A2). The simplest form of the solutions is a monotonically increasing function with respect to x and then

$$\int_{-m}^{u}\frac{d\eta}{\sqrt{F(-m)-F(\eta)}}=\sqrt{2}\left(x+\frac{l}{2}\right). \tag{A4}$$

The value m of u at the boundaries depends on the length l of the domain. A formula for m with l is given by letting $u=m$ in the limit of the integral and $x=l/2$. Since $F(u)$ is an even function, we obtain

$$l=\sqrt{2}\int_0^m\frac{d\eta}{\sqrt{F_m-F(\eta)}}, \quad F_m=F(-m)=\frac{m^2}{2}-\frac{m^4}{4},$$

$$=\sqrt{2}\int_0^m\frac{2d\eta}{\sqrt{(\eta^2-\mu^2)(\eta^2-\nu^2)}},$$

$$\mu^2=1-\sqrt{1-4F_m}=m^2,$$

$$\nu^2=1+\sqrt{1-4F_m}=2-m^2,$$

$$=\sqrt{2}\int_0^1\frac{2d\xi}{\nu\sqrt{(1-\xi^2)(1-k^2\xi^2)}},$$

$$\xi=\frac{\eta}{\mu}, \quad k^2=\frac{\mu^2}{\nu^2}=\frac{m^2}{2-m^2}, =\frac{2\sqrt{2}}{\sqrt{2-m^2}}K(k),$$

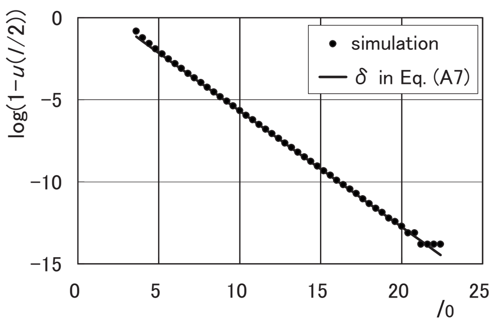

FIG. 9. Boundary value of the stationary standing front vs domain length l. Plotted are $\ln[1-u(l/2)]$ of simulation results (solid circles) and δ in Eq. (A7) (solid line).

$$K(k) = \int_0^1 \frac{d\xi}{\sqrt{(1-\xi^2)(1-k^2\xi^2)}} = \int_0^{\pi/2} \frac{d\xi}{\sqrt{1-k^2\sin^2\theta}}, \tag{A5}$$

where $K(k)$ is the complete elliptic integral of the first kind [29]. When l is large and m is close to unity, Eq. (A5) is approximated as [30]

$$l \approx \frac{2\sqrt{2}}{\sqrt{2-m^2}}\frac{1}{2}\ln\frac{16}{1-k^2}, \quad K(k) \to \ln\frac{4}{\sqrt{1-k^2}}, \quad k \to 1_-,$$

$$\approx \sqrt{2}\ln\left(\frac{1-m^2/(2-m^2)}{16}\right), \quad m \approx 1, \tag{A6}$$

$$m = \sqrt{2 - \frac{1}{1-8\exp(-l/\sqrt{2})}} \approx 1-\delta, \tag{A7}$$

$$\delta = 4\exp\left(\frac{-l}{\sqrt{2}}\right), \quad l \gg 1.$$

Thus m approaches to unity exponentially with l. This agrees with the standing front solution in an infinite domain in Eq. (2).

Figure 9 plots $\ln[1-u(l/2)]$ against l obtained with computer simulation using the initial condition

$$\varphi(x) = -1 \quad (-l/2 < x < 0)$$
$$= 1 \quad (0 \leqslant x < l/2). \tag{A8}$$

The method of the simulation is the same as in Sec. II. The solution satisfies the condition $u(-x,t) = -u(x,t)$ for all $t > 0$ and converges to the unstable stationary front solution. The value of $1-u(l/2)$ decreases exponentially as the domain length l increases. The value δ in Eq. (A7) (solid line) agrees with the simulation results (solid circles).

By letting $m=0$ in Eq. (A5), the smallest length $l_{\min}$ is given by $l_{\min} = 2K(0) = \pi$. Then such a standing front solution never exists in a domain of length less than π. Further, according to the boundary conditions in Eqs. (1) and (A1), solutions connecting $-m$ and m alternately can be constructed. Then there are stationary standing solutions up to the number $l/l_{\min}$ in a domain of length l. These stationary solutions are unstable and small fluctuations make the fronts move so that they annihilate each other [15,16].

2. Instantaneous speeds of fronts

Consider a general case in which $m_+ \neq -m_-$ in Eq. (A1). The speed of the stable traveling front in an infinite domain in Eq. (2) is derived by letting $z = x - ct$ in Eq. (1) [1–4]:

$$d^2u/dz^2 + c\,du/dz + f(u) = 0, \quad u(x,t) = u(z), \quad z = x - ct. \tag{A9}$$

By multiplying du/dz and integrating from $-\infty$ to ∞, Eq. (A9) leads to

$$\int_{-\infty}^{\infty} [(du/dz)(d^2u/dz^2) + c(du/dz)^2 + (du/dz)f(u)]dz = 0,$$

$$c = -\int_{-\infty}^{\infty}[f(u)du/dz]dz \Big/ \int_{-\infty}^{\infty}(du/dz)^2 dz$$
$$= -\int_{u(-\infty)}^{u(\infty)} f(u)du \Big/ \int_{-\infty}^{\infty}(du/dz)^2 dz. \tag{A10}$$

For a bounded domain $-l/2 < x < l/2$ in Eqs. (1) and (A1), this expression is still valid for front-type solutions by replacing the limits of the integrals with the values at the boundaries as

$$c = -\int_{m_-}^{m_+} f(u)du \Big/ \int_{-l/2}^{l/2}(du/dz)^2 dz, \tag{A11}$$

$$m_- = u(-l/2), \quad m_+ = u(l/2).$$

Although any traveling front solutions of nonzero speeds never exist perpetually in a fixed bounded domain, they can exist if the boundaries move at the same speed. Then the value of c in Eq. (A11) can be regarded as an instantaneous speed of a transient front connecting m_- and m_+.

Values of m_- and m_+ are necessary to obtain the speed c. When m_+ and $-m_-$ are the same, they depend on the domain length l with Eqs. (A5)–(A7). We here apply Eq. (A7) to the case in which $m_+ \neq -m_-$. Let l_+ be the length of the right domain in which $u > 0$ and then $l - l_+$ be the length of the left domain for $u < 0$ ($u < 0$ for $-l/2 < x < l/2 - l_+$ and $u > 0$ for $l/2 - l_+ < x < l/2$). The integral in the numerator in the right-hand side of Eq. (A11) is approximated as

$$\int_{m_-}^{m_+} f(u)du = \left[\frac{-u^4}{4} + \frac{u^2}{2}\right]_{m-}^{m+} \approx \delta_-^2 - \delta_+^2, \quad l \gg 1,$$

$$\delta_- = m_- + 1 = 4\exp[(l - l_+)/\sqrt{2}], \tag{A12}$$

$$\delta_+ = 1 - m_+ = 4\exp(-l_+/\sqrt{2}).$$

Note that $2l_+$ and $2(l - l_+)$ are substituted for l in $\delta_\pm$ since l_+ and $l - l_+$ correspond to the half length $l/2$. The integral in the denominator is approximated using the stable traveling front solution in Eq. (2) as

$$\int_{-l/2}^{l/2}(du/dz)^2dz \approx \int_{-l/2}^{l/2}\left(\frac{d\tanh(2^{-1/2}z)}{dz}\right)^2 dz = \frac{1}{\sqrt{2}}\left[\tanh\left(\frac{z}{\sqrt{2}}\right)-\frac{1}{3}\tanh^3\left(\frac{z}{\sqrt{2}}\right)\right]_{-l/2}^{l/2} \approx \sqrt{8/9} \quad (\approx 0.943), \quad l \gg 1. \tag{A13}$$

Hence, the movement of the front is expressed as

$$dl_+/dt = -c \approx 16\{\exp[-2(l-l_+)/\sqrt{2}] - \exp(-2l_+/\sqrt{2})\}/\sqrt{8/9} = k\{\exp[-\alpha(l-l_+)] - \exp(-\alpha l_+)\},$$

$$k = 24/\sqrt{2} \approx 17.0, \quad \alpha = 2\sqrt{2} \approx 2.83. \tag{A14}$$

This derivation also relates the values of u at the boundaries to the front speeds.

[1] D. G. Aronson and H. F. Weinberger, in *Partial Differential Equations and Related Topics*, edited by A. Dold and B. Eckmann, Lecture Notes in Mathematics Vol. 446 (Springer, Berlin, 1975).
[2] P. C. Fife, *Mathematical Aspects of Reacting and Diffusing Systems, Lecture Notes in Biomathematics*, Vol. 28 (Springer, Berlin, 1979).
[3] D. S. Jones and B. D. Sleeman, *Differential Equations and Mathematical Biology* (George Allen & Unwin, London, 1983).
[4] J. D. Murray, *Mathematical Biology* (Springer, Berlin, 1989).
[5] S. K. Scott and K. Showalter, J. Phys. Chem. **96**, 8702 (1992).
[6] M. C. Cross and P. C. Hohenberg, Rev. Mod. Phys. **65**, 851 (1993).
[7] F. Schlögl, C. Escher, and R. S. Berry, Phys. Rev. A **27**, 2698 (1983).
[8] A. Vl. Gurevich, S. L. Leikin, and R. G. Mints, Phys. Lett. **105A**, 31 (1984).
[9] A. S. Mikhailov, L. Schimansky-Geier, and W. Ebeling, Phys. Lett. **91A**, 453 (1983).
[10] A. Engel, Phys. Lett. **113A**, 139 (1985).
[11] J. P. Keener, SIAM J. Appl. Math. **47**, 556 (1987).
[12] J. A. Sherratt and B. P. Marchant, IMA J. Appl. Math. **56**, 289 (1996).
[13] R. Laister, A. T. Peplow, and R. E. Beardmore, Appl. Math. Lett. **17**, 561 (2004).
[14] A. Zlatoš, J. Am. Math. Soc. **19**, 251 (2006).
[15] K. Kawasaki and T. Ohta, Physica A **116**, 573 (1982).
[16] J. Carr and R. L. Pego, Commun. Pure Appl. Math. **42**, 523 (1989).
[17] S. Ei and T. Ohta, Phys. Rev. E **50**, 4672 (1994).
[18] M. J. Ward, SIAM J. Appl. Math. **56**, 1247 (1996).
[19] T. Nagai and K. Kawasaki, Physica A **120**, 587 (1983).
[20] K. Kawasaki and T. Nagai, Physica A **121**, 175 (1983).
[21] K. Kaneko, Phys. Lett. A **149**, 105 (1990).
[22] A. Wacker, S. Bose, and E. Schöll, Europhys. Lett. **31**, 257 (1995).
[23] U. Bastolla1 and G. Parisi, J. Phys. A **31**, 4583 (1998).
[24] R. Zillmera, R. Livib, A. Politic, and A. Torcini, Neurocomputing **70**, 1960 (2007).
[25] J. Šíma and P. Orponen, Theor. Comput. Sci. **306**, 353 (2003).
[26] T. Ishii and H. Kitajima, Proceedings of the 2006 RISP International Workshop on Nonlinear Circuits and Signal Processing, edited by T. Yahagi (unpublished); H. Kitajima, T. Ishii, and T. Hattori, Proceedings of the 2006 International Symposium on Nonlinear Theory and its Applications, edited by G. Setti and T. Ushio (unpublished); H. Kitajima and Y. Horikawa, Proceedings of the 2007 International Symposium on Nonlinear Theory and its Applications, edited by L. Trajkovic and K. Okumura (unpublished); Y. Horikawa and H. Kitajima, in *Noise and Fluctuations*, edited by M. Tacano *et al.*, AIP Conf. Proc. No. 922 (AIP, Melville, NY, 2007), p. 569.
[27] Y. Horikawa and H. Kitajima, Proceedings of the 2008 International Symposium on Nonlinear Theory and its Applications, edited by G. Kolumban and T. Endo (unpublished); Physica D (to be published).
[28] A. J. Bray, Adv. Phys. **51**, 481 (2002).
[29] S. Moriguchi, K. Udagawa, and S. Hitotsumatsu, *Mathematical Formulae* (Iwanami, Tokyo, 1956), Vols. I–III (in Japanese).
[30] I. S. Gradshteyn and I. M. Ryzhik, *Table of Integrals, Series, and Products*, 6th ed. (Academic, New York, 2000).
[31] Y. Horikawa, Proceedings of the 2008 International Symposium on Nonlinear Theory and its Applications, edited by G. Kolumban and T. Endo (unpublished).
[32] N. S. Goel and N. Richter-Dyn, *Stochastic Models in Biology* (Academic, New York, 1974).